NRC Research Press

ARTICLE

Climate-sensitive self-thinning trajectories of Chinese fir plantations in south China

Xiongqing Zhang, Lele Lu, Quang V. Cao, Aiguo Duan, and Jianguo Zhang

Abstract: The self-thinning rule is fundamental in regulating maximum stocking and constructing stand density management diagrams. Chinese fir (*Cunninghamia lanceolata* (Lamb.) Hook.) is the most important tree species and widely distributed across subtropical China. Yet, our understanding of how the self-thinning line of Chinese fir relates to climate is limited. Longitudinal data from 48 plots distributed in Fujian, Jiangxi, Guangxi, and Sichuan provinces were used to describe self-thinning for Chinese fir in relation to climate through first-order autoregressive (AR(1)) and nonlinear mixed effects (NLME) models. Results showed that self-thinning lines had steeper slopes for Chinese fir growing in areas with larger annual precipitation and summer mean maximum temperature but flatter slopes with higher mean annual temperature, degree-days below 0 °C, and winter mean minimum temperature. Winter mean minimum temperature was the dominant climatic factor in shaping self-thinning lines, which suggests that temperature was the key climate driver that affects self-thinning of Chinese fir. In addition, differences of slopes for any two of the four sites were significant, except between the Guangxi and Sichuan sites. Our results will be useful for both the silvicultural practices and mitigation strategies of Chinese fir under climate change in south China.

Key words: nonlinear mixed-effects model, hierarchical partitioning, self-thinning line, climate sensitive, Chinese fir.

Résumé : La loi de l'autoéclaircie est fondamentale pour réguler la densité maximum et construire les diagrammes de gestion de la densité des peuplements. Le sapin de Chine (*Cunninghamia lanceolata* (Lamb.) Hook.) est l'espèce d'arbre la plus importante et largement distribuée à travers la Chine subtropicale. Malgré cela, notre compréhension de la façon dont la courbe d'autoéclaircie du sapin de Chine est reliée au climat est déficiente. Des données longitudinales provenant de 48 placettes réparties dans les provinces du Fujian, Jiangxi, Guangxi et Sichuan ont été utilisées pour décrire l'autoéclaircie chez le sapin de Chine en lien avec le climat à l'aide de modèles autorégressifs du premier ordre et non linéaires à effets mixtes. Les résultats montrent que les courbes d'autoéclaircie ont une pente plus prononcée chez le sapin de Chine qui croît dans les régions où la précipitation annuelle et la température maximum moyenne durant l'été sont plus élevées, mais plus faibles où la température moyenne annuelle, les degrés-jours inférieurs à 0 °C et la température minimum moyenne sont plus élevés. La température minimum moyenne durant l'hiver était le facteur climatique qui influençait le plus les courbes d'autoéclaircie, ce qui indique que la température est le facteur climatique déterminant de l'autoéclaircie chez le sapin de Chine. De plus, les différences de pentes entre n'importe quelle paire parmi les quatre sites étaient significatives sauf entre les sites de Guangxi et Sichuan. Nos résultats seront utiles tant pour les pratiques sylvicoles que pour les stratégies visant à atténuer l'impact du changement climatique chez le sapin de Chine dans le sud de la Chine. [Traduit par la Rédaction]

Mots-clés : modèle non linéaire à effets mixtes, répartition hiérarchique, courbe d'autoéclaircie, sensible au climat, sapin de Chine.

Introduction

The self-thinning rule (Reineke 1933; Yoda 1963), which describes mortality induced by competing for light, water, and nutrients among trees within even-aged stands, continues to attract forest researchers' attentions (Bi 2004; Comeau et al. 2010; Burkhart 2013; Zhang et al. 2016). In forestry, the self-thinning rule has been applied in many areas such as developing relative density indices (Drew and Flewelling 1979; Woodall et al. 2005), predicting forest growth and yield (Smith and Hann 1986; Mäkelä et al. 2000; Pretzsch and Biber 2005), and establishing yield tables (Mesfin and Sterba 1996; Lhotka and Loewenstein 2008). The self-thinning rule is critical in constructing stand density management diagrams for many commercial species as a tool for deriving density-control schedules by management objective (Bégin et al. 2001; Newton 2012).

Since the late 1980s, the debate has primarily focused on whether the slope of the self-thinning line is constant (Zeide 1987; Bi and Turvey 1997; Pretzsch 2006; Zhang et al. 2016). A number of authors (Tang et al. 1995; Poage et al. 2007) support the notation that Reinke's slope is independent of site or environment conditions; however, this has been questioned by many authors. Several studies suggested that the slope of the self-thinning line may not be universally invariant and may vary depending on planting density (e.g., Turnblom and Burk 2000; VanderSchaaf and Burkhart

Received 22 April 2018. Accepted 23 July 2018.

X. Zhang, A. Duan, and J. Zhang. State Key Laboratory of Tree Genetics and Breeding, Research Institute of Forestry, Chinese Academy of Forestry, Beijing 100091, P. R. China; Collaborative Innovation Center of Sustainable Forestry in Southern China, Nanjing Forestry University, Nanjing, 210037, P. R. China; Key Laboratory of Tree Breeding and Cultivation of the State Forestry Administration, Research Institute of Forestry, Chinese Academy of Forestry, Beijing, 100091, P. R. China.
L. Lu. State Key Laboratory of Tree Genetics and Breeding, Research Institute of Forestry, Chinese Academy of Forestry, Beijing 100091, P. R. China; Key Laboratory of Tree Breeding and Cultivation of the State Forestry Administration, Research Institute of Forestry, Chinese Academy of Forestry, Beijing, 100091, P. R. China.
Q.V. Cao. School of Renewable Natural Resources, Louisiana State University Agricultural Center, Baton Rouge, LA 70803, USA.
Corresponding author: Jianguo Zhang (email: zhangjg@caf.ac.cn).

2007), site quality (e.g., Harper 1977; Pittman and Turnblom 2003; Weiskittel et al. 2009), nutrient availability (e.g., White and Solbrig 1980; Morris 2003; Reyes-Hernandez et al. 2013), climate (e.g., Deng et al. 2006; Comeau et al. 2010; Kweon and Comeau 2017), or biotic interactions (e.g., Zhang et al. 2011). Pretzsch (2002) reported that substantial differences in environment may affect size–density relationships and self-thinning trends. Brunet-Navarro et al. (2016) reported that self-thinning lines were species specific and affected by climatic conditions. Determining maximum stand density is crucial for both silvicultural practices and developing forest growth models. Clear information about the self-thinning rule under given climatic conditions can significantly contribute to the development of regionally appropriate and more precise silvicultural guidelines for constructing stand density management diagrams (Burkhart 2013; Condés et al. 2017).

Chinese fir (*Cunninghamia lanceolata* (Lamb.) Hook.), a fast-growing evergreen coniferous tree, is one of the most important tree species for timber production in south of China. As a native species, Chinese fir has been widely planted for over 1000 years. It produces high-quality timber with straight shape, high resistance of bending and cracking, and easily processing trait. Because of its commercial value, the planting area of Chinese fir in China is approximately 9.215 million ha, accounting for 28.54% of all forested land (Zhang et al. 2013). Zhang et al. (2016) used a linear—quadratic–linear segmented model to simulate the self-thinning trajectories of Chinese fir plantations and found that the self-thinning slope was invariant with changes in planting densities but different in sites of subtropical zones. There remains a need to explore whether the self-thinning trajectories of Chinese fir are influenced by climatic conditions. If self-thinning lines are sensitive to climatic variables, they could be used as a tool to evaluate climate change adaptation and mitigation strategies.

The next logical step to the study by Zhang et al. (2016) should be to see if climatic variables can be included in the self-thinning model, so that a single model can be used to describe stand behavior in various locations. The objectives of this study are as follows: (*i*) to determine whether the self-thinning trajectories of Chinese fir in south China are affected by climatic conditions; (*ii*) to identify the contributions of climatic factors to the self-thinning trajectories; (*iii*) to develop a climate-sensitive self-thinning model. The findings will be useful for developing both silvicultural practices and mitigation strategies of Chinese fir under climate change in south China.

Materials and methods

Study sites and self-thinning data

Data for this study were from Chinese fir stands established using bare-root seedlings in 1982 in three provinces (sites) in southern China: Fujian, Guangxi, and Sichuan (Fig. 1), and in 1981 in Jiangxi province. The study site located in Guangxi has a southern subtropical climate, whereas other sites in Fujian, Jiangxi, and Sichuan have a middle subtropical climate. Most Chinese fir trees grow in the subtropical zone in southern China (Fig. 1). In each site, the plots were planted in a randomized block design with repeated measurements with the following tree spacings: 2 m × 1.5 m (3333 trees·ha^{-1}), 2 m × 1 m (5000 trees·ha^{-1}), 1 m × 1.5 m (6667 trees·ha^{-1}), and 1 m × 1 m (10 000 trees·ha^{-1}). Each spacing level was replicated three times. There are 12 plots per site, i.e., 4 spacement × 3 replications. Each plot comprised a 20 m × 30 m area and a buffer zone consisting of two rows of similarly treated trees surrounding each plot. Diameters at breast height (1.3 m, DBH) of all trees in the plots were measured after tree heights reached 1.3 m in the first winter and every 2 or 3 years afterward. In the winter of 1998, there was a snow storm in Jiangxi, resulting in numerous dead trees. We therefore excluded the data after 1999 from Jiangxi. The trajectories of stand density in terms of number of trees per hectare (*N*) and quadratic mean diameter (*Q*) are shown for each site in Fig. 2, and the summary statistics for *Q* and *N* by site are described in Table 1.

Candidate climate variables

Each site was characterized by a set of climatic variables: minimum, mean and maximum mean monthly temperatures, mean warmest and coldest monthly temperatures, total and seasonal precipitation, etc. Because real climate data of study sites were lacking, we obtained these variables across the sites based on ClimateAP (Wang et al. 2012). ClimateAP is a climate data downscaling tool, which produces directly calculated seasonal and annual climate variables and derives climate variables for specific locations (scale-free) based on latitude, longitude, and elevation (Zhang et al. 2017). However, climate records in ClimateAP were only up to 2012, and we obtained the climate data of 2013 in Naxi from National Meteorological Observing Station of China. Both temperature and precipitation affect the physiological and growth processes of plant species (Leites et al. 2012; Żywiec et al. 2017). Some reports mentioned that heat, water supply, and winter coldness may be key limitation factors causing tree death (e.g., Worrall et al. 2013; Camarero et al. 2015). According to both literature and preliminary analyses, we selected a subset of climatic variables across the study sites most relevant to self-thinning for the Chinese fir plantations. The selected variables were mean annual temperature (MAT), annual precipitation (AP), mean warmest monthly temperature (MWMT), mean coldest monthly temperature (MCMT), degree-days below 0 °C (DD_0), summer mean maximum temperature (SMMT), winter mean minimum temperature (WMMT), and spring mean temperature (SMT). The annual heat—moisture index (AHM = (MAT + 10)/(AP/1000)), an inverse form of the De Martonne aridity index (De Martonne 1926), was used to indicate the annual heat and water supply (Rehfeldt et al. 1999). This index better reflects evapotranspiration and soil moisture content than precipitation and temperature alone (Zhang et al. 2014). Large values of AHM indicate dry conditions, whereas low values of AHM represent relatively wet conditions. The summary statistics of climatic variables across the study sites are shown in Table 2.

Modeling climate-dependent self-thinning line

Within early stages of monospecific plantations, stand density does not affect mortality because intraspecific competition for limited resources such as light, water, and nutrients has not yet started. The trajectory is close to a horizontal line. When trees continue to increase in size, some trees must die and the density-dependent death begins. The segmented regression technique (Gallant and Fuller 1973) has the ability to describe complicated functional forms and has been applied in modeling self-thinning trajectories (Cao and Dean 2008; VanderSchaaf and Burkhart 2008). Zhang et al. (2016) used the following segment model to describe the self-thinning trajectories of Chinese fir:

$$y_2 = y_1 + b\left[(x_2 - a_{11} - a_{12}y_0)^2 I_{12} - \left(x_2 - a_{11} - a_{12}y_0 - \frac{c}{2b}\right)^2 I_{22} - (x_1 - a_{11} - a_{12}y_0)^2 I_{11} + \left(x_1 - a_{11} - a_{12}y_0 - \frac{c}{2b}\right)^2 I_{21}\right] + \varepsilon \quad (1)$$

where

$$I_{1i} = \begin{cases} 1, & \text{if } x_i > a_{11} + a_{12}y_0 \\ 0, & \text{otherwise} \end{cases}$$

$$I_{2i} = \begin{cases} 1, & \text{if } x_i > a_{11} + a_{12}y_0 + \dfrac{c}{2b} \\ 0, & \text{otherwise} \end{cases}$$

and where $i = 1, 2$, x_i and y_i are values of ln(*Q*) and ln(*N*) at time *i*, respectively, $i = 1, 2$; $y_0 = \ln(N_0)$; N_0 is planting density; b, c, a_{11}, and a_{12} are regression parameters; c is slope of the self-thinning line; and ε is random error. Although Zhang et al. (2016) found that eq. 1

Fig. 1. Locations of the study site consisting of three subtropical climate zones.

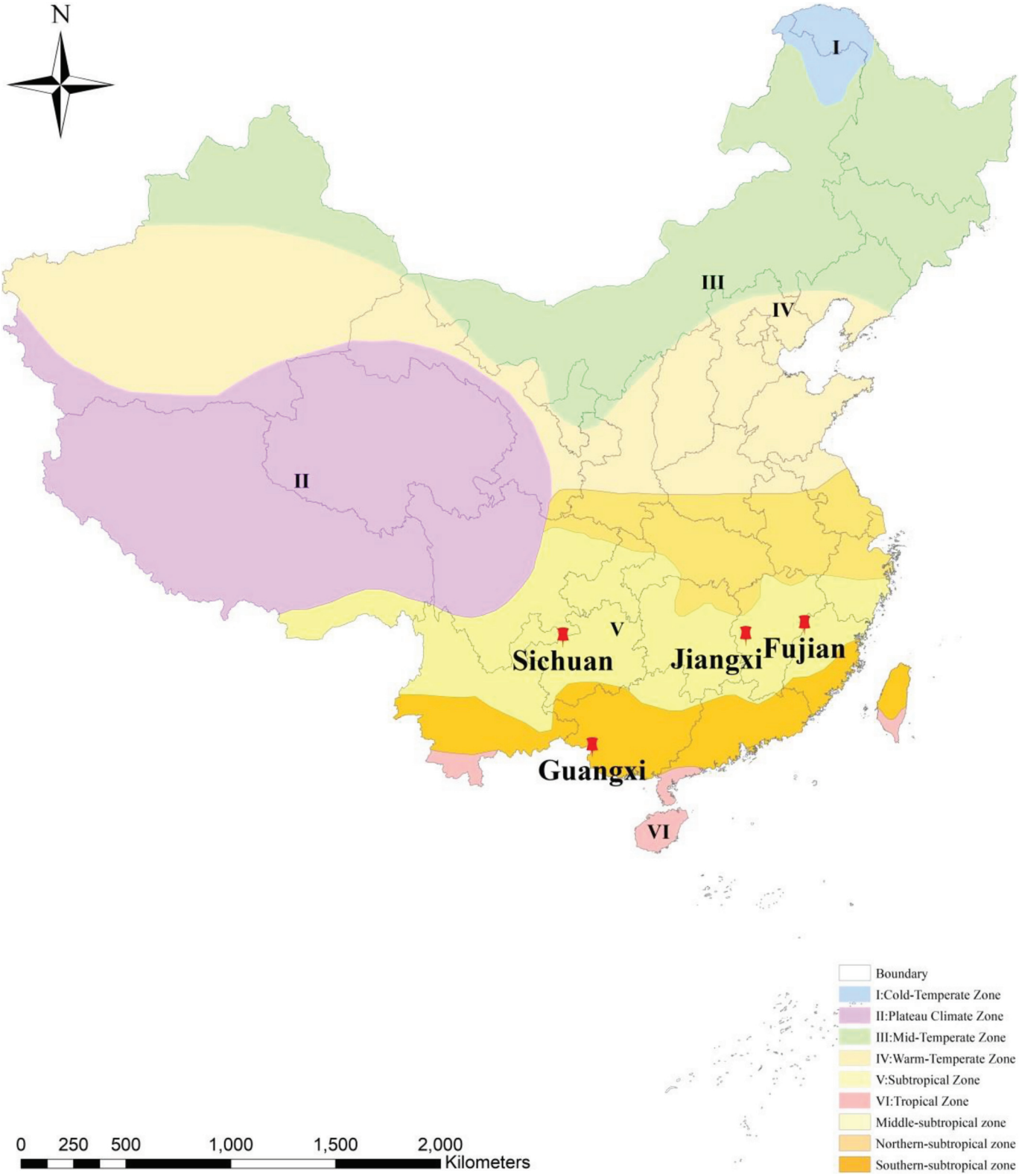

performed well on modeling self-thinning trajectories of Chinese fir, they did not take into account whether or not the self-thinning trajectories were affected by climatic conditions. To explore the effects of climatic variables on self-thinning trajectories in this study, the slope c in eq. 1 was re-parameterized by using climatic variables:

$$c = f(\mathrm{Clim}_i) \quad (2)$$

where Clim_i is the climatic variables for time i listed in Table 2. Two methods were explored to account for the autocorrelation among repeated measurements from the same plot: first-order autoregressive model, AR(1),

Fig. 2. Relationship between the log of stand density (*N*) and quadratic mean diameter (*Q*) by site.

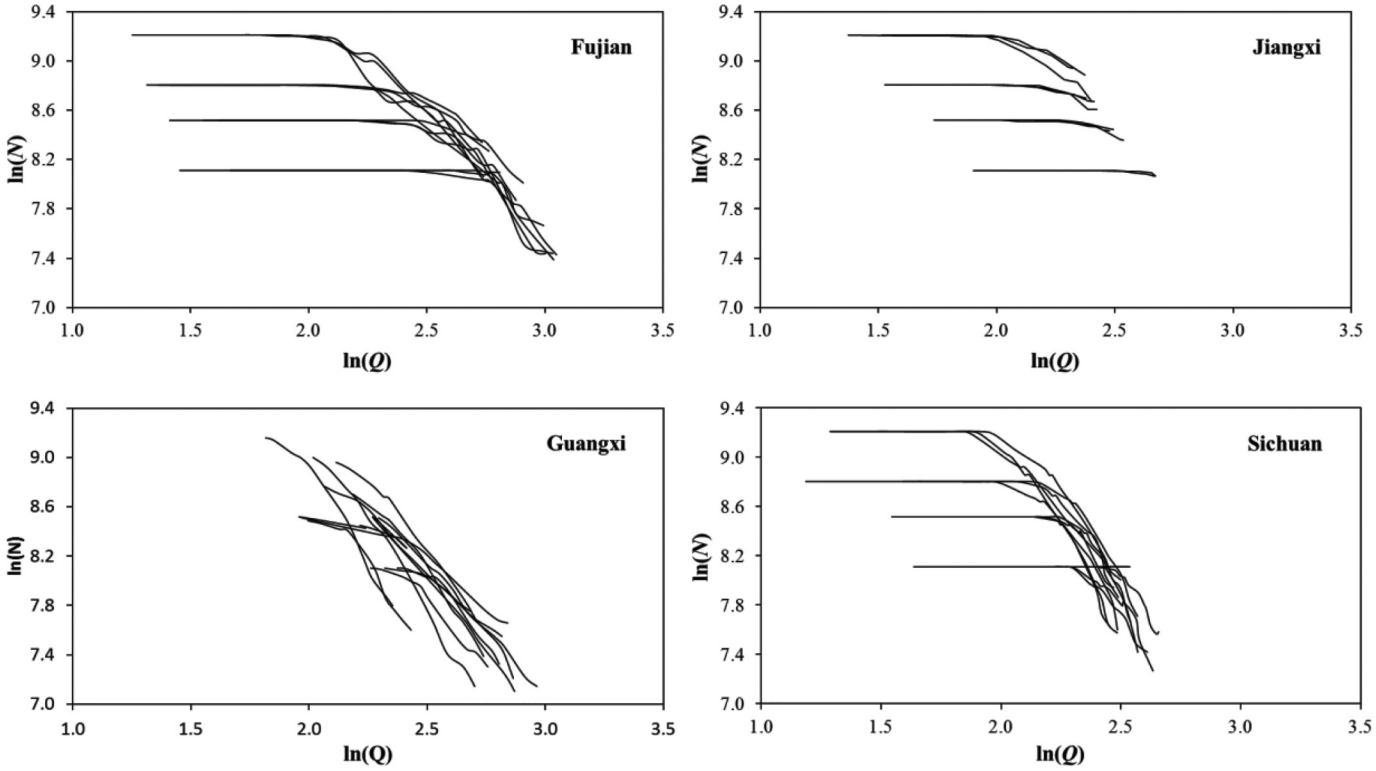

Table 1. Coordinates, soil type, measurement years, and summary statistics for stand quadratic mean diameter (*Q*, in cm) and number of trees per hectare (*N*) by site.

						Q		*N*	
Site	Coordinates	Soil type	No. of plots	Measurement year	*n*	Mean	SD	Mean	SD
Fujan	27°05′N 117°43′E	Laterite	12	Every year during 1985–1990; every 2 years during 1990–2010	192	11.26	4.35	5120	2262.45
Jiangxi	27°30′N 114°33′E	Laterite, yellow	12	Every year during 1985–1989; every 2 years during 1989–1999	124	9.20	2.47	5977	2237.00
Guangxi	22°06′N 106°43′E	Laterite	12	Every year during 1990–1995; every 2 years during 1995–2009	132	11.82	2.90	3627	1815.02
Sichuan	28°47′N 105°23′E	Laterite	12	Every year during 1985–1995; every 2 or 3 years during 1995–2013	192	9.70	2.42	4646	2212.24

Note: *n*, total number of measurements for all plots; SD, standard deviation.

Table 2. Summary statistics of climate variables.

	Fujian		Jiangxi		Sichuan		Guangxi	
Climate variable	Mean	SD	Mean	SD	Mean	SD	Mean	SD
MAT (°C)	18.96	0.47	18.19	0.38	18.43	0.37	22.11	0.41
MWMT (°C)	28.22	0.66	28.21	0.76	28.2	0.80	28.15	0.45
MCMT (°C)	8.58	1.06	7.13	1.05	8.21	1.00	13.65	1.08
AP (mm)	1809.53	260.62	1673.13	209.07	1164.43	126.67	1465.14	238.25
AHM	16.25	2.09	17.09	2.08	24.72	2.93	22.42	3.27
DD_0	1.41	0.62	2.6	0.91	1.64	0.62	0	0
SMMT (°C)	32.19	0.50	31.99	0.77	30.61	0.66	31.68	0.49
WMMT (°C)	4.85	0.78	4.42	0.85	7.21	0.65	11.96	0.77
SMT (°C)	18.43	0.87	17.46	0.69	18.68	0.58	22.65	0.56

Note: MAT, mean annual temperature; MWMT, mean warmest month temperature; MCMT, mean coldest month temperature; AP, annual precipitation; AHM, annual heat–moisture index; DD_0, degree-days below 0 °C, chilling degree-days; SMMT, summer (June–August) mean maximum temperature; WMMT, winter (December (of previous year)–February) mean minimum temperature; SMT, spring (March–May) mean temperature.

Fig. 3. The mean annual temperature (MAT) and annual precipitation (AP) curves by year in four sites. [Colour online.]

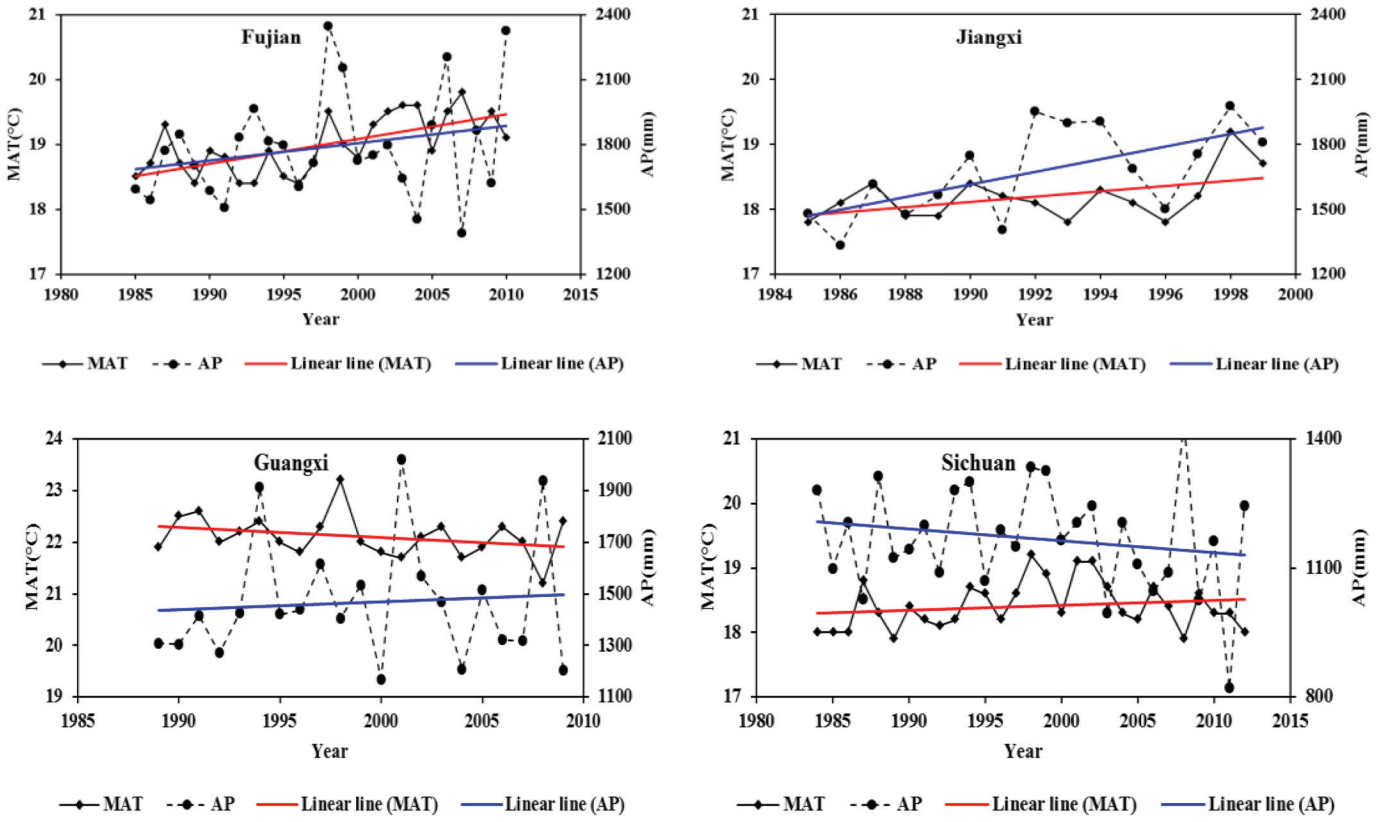

$$(3)\quad \begin{cases} y_2 = y_1 + b\left[(x_2 - a_{11} - a_{12}y_0)^2 I_{12} - \left(x_2 - a_{11} - a_{12}y_0 - \frac{c}{2b}\right)^2 I_{22} - (x_1 - a_{11} - a_{12}y_0)^2 I_{11} + \left(x_1 - a_{11} - a_{12}y_0 - \frac{c}{2b}\right)^2 I_{21}\right] + \mu_t \\ \mu_t = \phi\mu_{t-1} + \varepsilon_t \\ c = f(\mathrm{Clim}_i) \end{cases}$$

and nonlinear mixed-effects model (NLME)

$$(4)\quad \begin{cases} y_2 = y_1 + (b + v)\left[(x_2 - a_{11} - a_{12}y_0)^2 I_{12} - \left(x_2 - a_{11} - a_{12}y_0 - \frac{c}{2b}\right)^2 I_{22} - (x_1 - a_{11} - a_{12}y_0)^2 I_{11} + \left(x_1 - a_{11} - a_{12}y_0 - \frac{c}{2b}\right)^2 I_{21}\right] + \varepsilon_t \\ c = f(\mathrm{Clim}_i) \end{cases}$$

where ϕ is regression parameter, and v is random-effect parameter specific to each individual plot and assumed to be to be normally distributed with mean 0 and variance σ^2. The AR(1) and NLME models were performed by use of SAS procedures MODEL and NLMIXED, respectively (SAS Institute, Inc. 2011). For the NLME model, the unstructured covariance method (Littell et al. 1996) was used for describing the variance–covariance structure of the random effect.

To avoid potential issues with multicollinearity, each climate variable was pre-selected by way of the variance inflation factor (VIF) test. A common rule of the test is that multicollinearity exists if VIF > 5. The VIF test was performed using SAS software (SAS Institute, Inc. 2011). Zhang et al. (2016) reported that the self-thinning trajectories from Jiangxi and Fujian were similar, and the likelihood ratio test confirmed that data from these two sites can be combined to fit the self-thinning equation. In this study, we modeled the self-thinning trajectory for each site (with data from Jiangxi and Fujian combined as one site) using the AR(1) and NLME methods. These methods are labeled AR(1)_NC and NLME_NC for models without climate variables and AR(1)_C and NLME_C for models with climate variables.

In addition, for identifying the contributions of selected climate variables to the self-thinning line, we used the hierarchical partitioning (HP), which calculates goodness of fit measures for the entire hierarchy of models using all combinations of independent variables and identify the average independent contribution of each variable to the model (Behrens et al. 1991; Chevan and Sutherland 1991). The HP analysis was performed using the hier.part package in R software (Nally and Walsh 2004; R Development Core Team 2015). Trends in climate variables were estimated using linear models.

Model evaluation

The following evaluation statistics of mean absolute difference (MAD) and R^2 were used to validate the AR(1) and NLME models:

$$(5)\quad \mathrm{MAD} = \frac{\Sigma|y_i - \hat{y}_i|}{n}$$

Table 3. Parameter estimates and model evaluation statistics using the AR(1) method without climatic variables (AR(1)_NC) and with climatic variables (AR(1)_C), as well as the nonlinear mixed-effects model with climatic variables (NLME_C) and without climatic variables (NLME_NC).

	AR(1)_NC				NLME_NC				
Parameter	Fujian and Jiangxi	Guangxi	Sichuan	AR(1)_C	Fujian and Jiangxi	Guangxi	Sichuan	All	NLME_C
a_{11}	7.27	6.13	7.05	7.58	7.20	6.46	4.92	6.64	6.67
a_{12}	−0.51	−0.43	−0.53	−0.56	−0.51	−0.47	−0.28	−0.46	−0.45
b	2.05	3.23	4.54	2.16	2.04	2.71	5.05	2.41	2.14
c	−2.44	−2.32	−3.26	—	−2.45	−2.40	−3.81	−2.42	—
c_0				−8.44					−13.74
c_1				−0.30					−0.24
c_2				0.0008					0.0011
c_3				−0.15					−0.17
c_4				0.33					0.45
c_5				—					−0.02
σ^2				—	0.0077	0.43	3.39	0.03	0.06
Evaluation statistics									
R^2	0.9920	0.9922	0.9917	0.9907	0.9923	0.9910	0.9943	0.9855	0.9917
MAD	0.0198	0.0345	0.0291	0.0284	0.0192	0.0332	0.0225	0.0368	0.0269

Note: All parameters were significantly different at level 0.05 other than σ^2 in the NLME_NC model. When combined, the R^2 and MAD (mean absolute difference between observed and predicted values) equals the goodness of fit, as models with lower MAD and larger R^2 values indicate a better fit to the data. "All" = all four sites together (pooled data).

$$R^2 = 1 - \frac{\Sigma(y_i - \hat{y}_i)^2}{\Sigma(y_i - \bar{y})^2} \quad (6)$$

where y_i is stand density for the ith observation, $\hat{y}_i$ and $\bar{y}$ are predicted value and average, respectively, of y_i, and n is number of observations. Models with lower MAD and higher R^2 values indicate a better fit to the data.

Results

Selection of climate variables

Based on the VIF test, we found that there was no multicollinearity (VIF < 5) among MAT, AP, DD_0, SMMT, and WMMT. The re-parameterized model for c is

$$c = c_0 + c_1(\text{MAT}) + c_2(\text{AP}) + c_3(\text{DD\_0}) + c_4(\text{SMMT}) + c_5(\text{WMMT}) \quad (7)$$

Figure 3 shows the changes of MAT and AP with time during the study period. Linear model analysis revealed that MAT showed a significant increase in Fujian (p = 0.0003), a moderate increase in Jiangxi (p = 0.0686), and no significant change in Guangxi and Sichuan (p = 0.1881 and 0.3798, respectively). On the other hand, AP increased significantly in Jiangxi (p = 0.0135) but showed no significant changes in Fujian, Guangxi, and Sichuan (p = 0.2222, 0.7307, and 0.3478, respectively).

Effects of climate on self-thinning slope

In the AR(1) model, MAT, AP, DD_0, and SMMT were significantly correlated (p < 0.05) with the slope c of the self-thinning line, whereas WMMT was not. In contrast, all of the climatic variables were significant at 0.05 level in the NLME model (Table 3). The slope of the self-thinning line increased with increasing AP and SMMT and decreased with increasing MAT, DD_0, and WMMT. This suggested a steeper slope for areas with larger AP and SMMT and a flatter slope for areas with higher MAT, DD_0, and WMMT.

Except for the Jiangxi site, the slopes were significantly different between models with and without climatic variables (Fig. 4), indicating that climate did affect the self-thinning line. Furthermore, the NLME model with climatic variables having larger R^2 value of 0.9917 and smaller MAD value of 0.0269 performed better than the model without climatic variables (0.9855 and 0.0368 for R^2 and MAD, respectively) using pooled data (Table 3).

The hierarchical partitioning analysis showed that WMMT contributed the most to stocking (49.93%), followed by MAT, DD_0, AP, and SMMT (Fig. 5). These results indicated that WMMT was the most important climate variable that contributed to self-thinning among the selected five climatic variables.

Comparing AR(1) with NLME

A t test showed that the mean of all slopes computing from four sites using the AR(1) model (−2.7504) was significantly different (p = 0.0273) from that using the NLME model (−3.0025). It means that the self-thinning line from the AR(1) model was flatter than the one from the NLME model. In Fujian, there was no significant difference (p = 0.3995) between slopes from the AR(1) and NLME models. We also found that both models performed well (R^2 > 0.99, Table 3) and the NLME model slightly better (larger R^2 and smaller MAD values, Table 3). Even though WMMT was the most important climate variable used to model the self-thinning line based on the hierarchical partitioning analysis, it was not significant at the 0.05 level in the AR(1) model. This suggests that the climate-sensitive NLME model was the best model for analyzing self-thinning trajectories of Chinese fir in south China.

Effects of site on slope

Based on the climate-sensitive NLME model, slopes in four sites were different (p < 0.01) according to repeated measures analysis of variance (RANOVA) analysis. Furthermore, the Tukey post-hoc test following the overall effect analysis of RANOVA revealed that the differences of slope between Guangxi and Sichuan were not significant (p > 0.05), but slopes from any two of the other sites were significantly different (p < 0.05, Fig. 4).

Discussion

The self-thinning line is a very useful tool in forestry. A single self-thinning line has routinely been used to describe all conditions at a regional scale (Reyes-Hernandez et al. 2013; Toïgo et al. 2015). However, the boundary lines varied among sites (or regions) for a given species (Brunet-Navarro et al. 2016; Charru et al. 2012). In this study, we fitted self-thinning models that explain this variability at different sites to provide self-thinning trajectories accordingly.

Fig. 4. Box plot of slope *c* of self-thinning line. Different letters indicate significant differences ($p < 0.05$) based on a Tukey post-hoc test following the overall effect analysis of RANOVA.

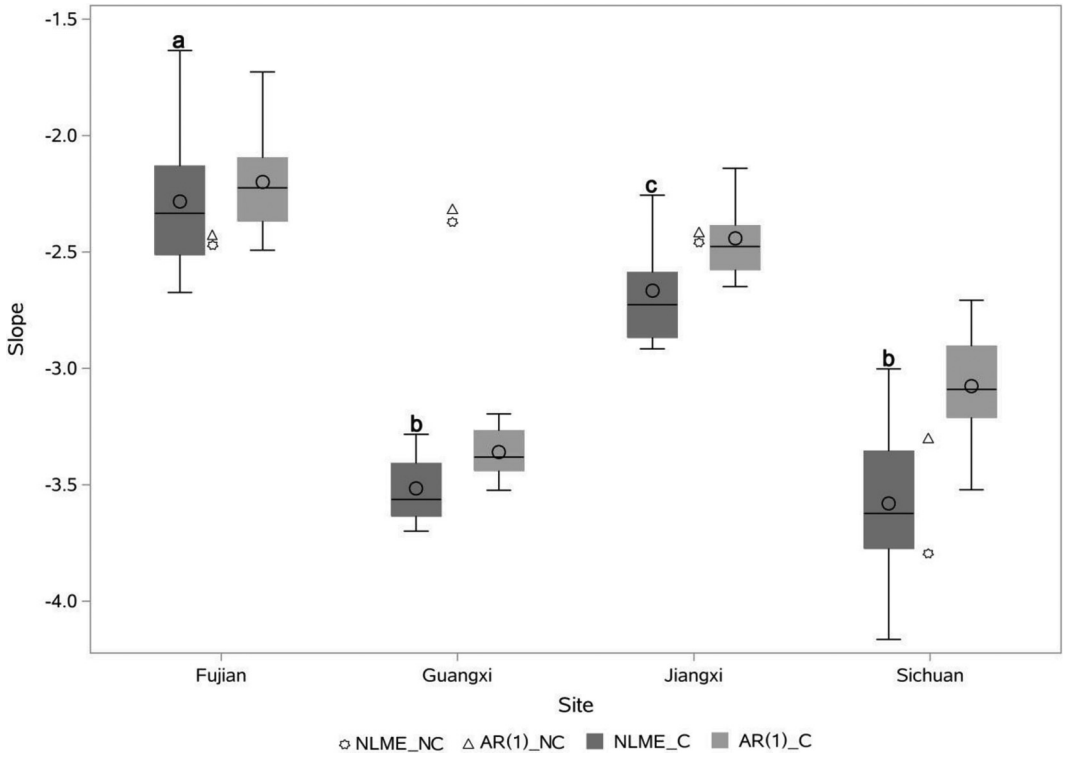

Fig. 5. Bar plot of relative importance contributed to self-thinning line through hierarchical partitioning analysis.

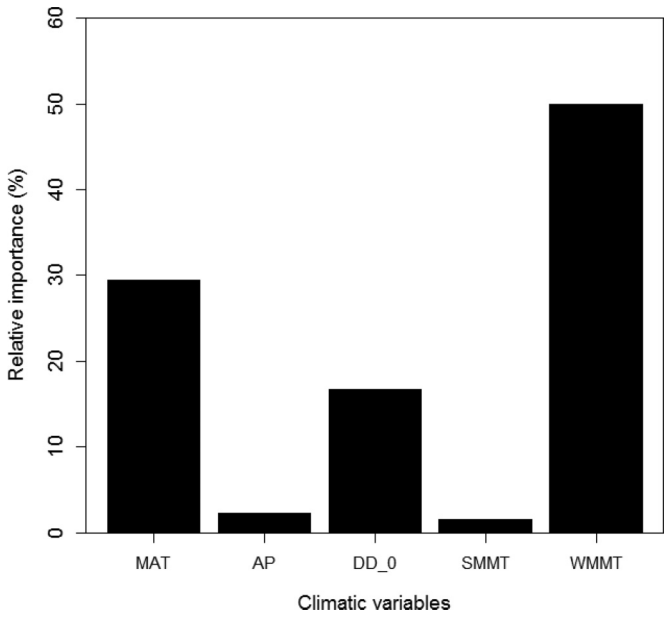

Effects of climate on self-thinning line

The self-thinning line was thought to reflect trees competition for resources such as light, nutrients, and water. Some authors found the slope of the self-thinning line increased at better sites (Zeide 1987). Reyes-Hernandez et al. (2013) proposed a new formulation of the self-thinning line that explicitly includes site quality indicators such as soil moisture and nutrient regimes. In this study, slope values of the self-thinning line decreased with increasing MAT, DD_0, and WMMT, which indicated that tree death decreased with increasing MAT, DD_0, and WMMT. However, some studies showed that rising temperature accelerated tree death (Mueller et al. 2005; Peng et al. 2011; Zhang et al. 2014). In general, an increasing MAT decreases tree death probabilities physiologically, when water availability is not limiting (Zhang et al. 2017). In addition, Chinese fir is a shade-intolerant tree species, the growth of which tends to increase with high temperature (Wu 1984), thus making the slope of the self-thinning line flatter. For sensitive species with extended growing season, higher values of DD_0 increased hardening, later dormancy, and risk of frost damage (Andrews 2016), resulting in tree death. This explains why the self-thinning lines from our study tended to be flatter in areas with larger DD_0 values (Table 3). A warm winter can extend the growing season, therefore increase radial growth and consequently stocking in the following year. The net result is the negative relationship between the WMMT and slope of the self-thinning line observed in this study. This was consistent with findings from a previous study (Kweon and Comeau 2017). It is also said that warmer winter can accelerate dryness in the growing season and reduce waterlogging.

Tree death was mainly attributed to wet and dry years (Schmidt-Vogt 1989), with wet years causing death of fine roots due to waterlogging (Vygodskaya et al. 2002), which in turn increased soil erosion, slope failure, and phytophthora infection. The self-thinning slope in water-stressed conditions was flatter than in well-watered conditions (Liu et al. 2006). Vizcaíno-Palomar et al. (2016) found that higher precipitation in some sites might imply poorer soil quality, because of increased runoff and nutrient leaching in the soils. In line with these results, we found that steeper slopes for Chinese fir occurred in wet areas (Table 3). In other regions, aridity was the primary explanation of limiting tree growth in tropical and lowland Mediterranean regions (Segura et al. 2003; Banin et al. 2012; Brunet-Navarro et al. 2016). Water stress may alter the size symmetry of competition, as well as the level of stress (Chu et al. 2010). However, in this study, the effect of AHM index on self-thinning line of Chinese fir was insignificant

($p > 0.05$), and this was removed in the final model. This might be because there was no water deficit in subtropical regions in this study.

Warm summers that results in increasingly severe soil moisture deficits would reduce tree growth and increase the likelihood of tree death (Neumann et al. 2017). Chinese fir tends to live in warmer conditions, but it is not resistant to overly high temperature. Too high of a temperature would result in enhancing heat stress and heat-induced moisture stress, consequently accelerating tree death. In this study, we found that the self-thinning line of Chinese fir had a steeper slope in areas with high SMMT (Table 3).

The dominant climatic factor in shaping the self-thinning line of Chinese fir was WMMT, followed by MAT, DD_0, AP, and SMMT (Fig. 5). These findings were consistent with those from previous studies that temperature was the dominant factor affecting forest structures in humid mountains or regions with moisture sufficiency (Weaver and Murphy 1990; Pendry and Proctor 1997). It indicated that temperature was a key climate driver that shape the self-thinning line of Chinese fir in subtropical China and provided the evidence that climate does have an influence on maximum stand stocking. Overall, the NLME model with climatic variables was superior to the one without climatic variables because of the spatial variability of climate (Table 3).

Comparison with previous studies

VanderSchaaf and Burkhart (2007) found that a mixed-effects model performed better than a first-difference model in estimating the self-thinning line. Consistent with this result, the climate-sensitive NLME model was superior to the AR(1) model for analyzing the self-thinning line of Chinese fir plantations in south of China. Zhang et al. (2016), without considering the climate effects on self-thinning, reported that there were no significant differences among slopes of the self-thinning lines of Chinese fir in the Fujian, Jiangxi, and Guangxi sites. Comeau et al. (2010) provided additional evidence that self-thinning lines were influenced by environmental and other factors and indicate the need for development of a self-thinning line for each region for a given species. Here, we incorporated the climate variables into the self-thinning line models and found that site effects on slope were significant. In addition, slopes in Guangxi and Sichuan were not significantly different. It is noted that the site quality in Guangxi and in Sichuan are lower than that in the other two sites (Wu 1984), which resulted in flatter slopes in Fujian and Jiangxi compared with those in Guangxi and Sichuan (Fig. 4).

Based on self-thinning data from 12 of 14 species, Reineke (1933) found that the self-thinning slope was –1.605. Many authors have since questioned this result. Rivoire and Le Moguedec (2012) reported that slopes of species such as oaks (*Quercus* spp.), common beech (*Fagus sylvatica* L.), and Norway spruce (*Picea abies* (L.) Karst.) varied between –1.605 and –1.85. Charru et al. (2012) also found that the slope was species dependent, ranging from –1.941 to –1.615 for 1 temperate species in France. Comeau et al. (2010) mentioned that slope of the same species was influenced by site: slopes of Sitka spruce (*Picea sitchensis* (Bong.) Carrière) were –2.063 in Great Britain and –1.437 in Western Canada, whereas slopes of Douglas fir (*Pseudotsuga menziesii* (Mirb.) Franco) in Great Britain and Western Canada were –1.864 and –1.241, respectively. Most of the slopes mentioned above were larger than –2. Slope values larger than –2 indicated an increase in maximum basal area with increasing quadratic mean diameter (Q) according to the pipe model theory (Shinozaki et al. 1964; Mäkelä and Valentine 2006). However, in this study, we found that slopes of the self-thinning lines (ranging from –4.1647 to –1.6355) were sensitive to climate, and slopes in four sites were smaller than –2, which suggested that the maximum basal area declined with increasing Q. This may be because the functional allometry of the trees changes (e.g., a substantial change in hydraulic architecture) with a decrease in resource availability or the efficiency of use of limiting resource with increasing size (Condés et al. 2017).

In addition, describing the size–density relationship in response to climate change is crucial for developing climate adaptation strategies. The results suggest that the self-thinning lines of Chinese fir were different in four sites and could be modeled by use of climate variables. Therefore, more attention should be paid to these factors when we control the level of growing stock of Chinese fir through either initial spacing or subsequent thinnings to achieve specific management objectives.

Conclusions

This study characterized the climate-sensitive self-thinning trajectories of Chinese fir plantations by use of the AR(1) model and the NLME model in four sites in south of China: Fujian, Jiangxi, Guangxi, and Sichuan. The climate-sensitive NLME model simulated the self-thinning trajectories of Chinese fir plantations well. Chinese fir growing in areas with larger AP and SMMT had a significantly steeper slope but had a flatter slope in areas with higher MAT, DD_0, and WMMT. The dominant climatic factor in shaping the self-thinning line of Chinese fir was WMMT, followed by MAT, DD_0, AP, and SMMT, which suggested that temperature was the dominant factor affecting self-thinning of Chinese fir in subtropical China. Differences of slopes in any two of the four sites were significant, except between the Guangxi and Sichuan sites. Overall, inclusion of climate variables in self-thinning models can facilitate projection of the size–density relationship under future climate change conditions.

Acknowledgements

The study was supported by the Fundamental Research Funds for the Central Non-profit Research Institution of CAF (CAFYBB2017ZX001-2), the National Natural Science Foundation of China (No. 31670634), and the Young Elite Scientists Sponsorship Program by CAST (No. 2017QNRC001). Partial support for data analysis was received from the National Institute of Food and Agriculture, U.S. Department of Agriculture, Mclntire-Stennis project LAB94223.

References

Andrews, C. 2016. Modeling and forecasting the influence of current and future climate on eastern North American spruce-fir (*Picea-Abies*) forests. M.Sc. thesis, University of Maine, Orono, Maine.

Banin, L., Feldpausch, T.R., Phillips, O.L., Baker, T.R., Lloyd, J., Affum-Baffoe, K., Arets, E.J.M.M., Berry, N.J., Bradford, M., Brienen, R.J.W., Davies, S., Drescher, M., Higuchi, N., Hilbert, D.W., Hladik, A., Iida, Y., Abu Salim, K., Kassim, A.R., King, D.A., Lopez-Gonzalez, G., Metcalfe, D., Nilus, R., Peh, K.S.H., Reitsma, J.M., Sonké, B., Taedoumg, H., Tan, S., White, L., Wöll, H., and Lewis, S.L. 2012. What controls tropical forest architecture? Testing environmental, structural and floristic drivers. Global Ecol. Biogeogr. **21**(12): 1179–1190. doi:10.1111/j.1466-8238.2012.00778.x.

Bégin, E., Bégin, J., Bélanger, L., Rivest, L.P., and Tremblay, S. 2001. Balsam fir self-thinning relationship and its constancy among different ecological regions. Can. J. For. Res. **31**(6): 950–959. doi:10.1139/x01-026.

Behrens, D., Harbich, K., and Barke, E. 1991. Hierarchical partitioning. Am. Stat. **45**(2): 90–96. doi:10.1080/00031305.1991.10475776.

Bi, H. 2004. Stochastic frontier analysis of a classic self-thinning experiment. Austral Ecol. **29**(4): 408–417. doi:10.1111/j.1442-9993.2004.01379.x.

Bi, H., and Turvey, N.D. 1997. A method of selecting data points for fitting the maximum biomass-density line for stands undergoing self-thinning. Austral Ecol. **22**(3): 356–359. doi:10.1111/j.1442-9993.1997.tb00683.x.

Brunet-Navarro, P., Sterck, F.J., Vayreda, J., Martinez-Vilalta, J., and Mohren, G.M.J. 2016. Self-thinning in four pine species: an evaluation of potential climate impacts. Ann. For. Sci. **73**(4): 1025–1034. doi:10.1007/s13595-016-0585-y.

Burkhart, H.E. 2013. Comparison of maximum size-density relationships based on alternate stand attributes for predicting tree numbers and stand growth. For. Ecol. Manage. **289**: 404–408. doi:10.1016/j.foreco.2012.10.041.

Camarero, J.J., Gazol, A., Sancho-Benages, S., and Sangüesa-Barreda, G. 2015. Know your limits? Climate extremes impact the range of Scots pine in unexpected places. Ann. Bot. **116**(6): 917–927. doi:10.1093/aob/mcv124. PMID: 26292992.

Cao, Q.V., and Dean, T.J. 2008. Using segmented regression to model the density-

size relationship in direct-seeded slash pine stands. For. Ecol. Manage. **255**(3–4): 948–952. doi:10.1016/j.foreco.2007.10.004.

Charru, M., Seynave, I., Morneau, F., Rivoire, M., and Bontemps, J.D. 2012. Significant differences and curvilinearity in the self-thinning relationships of 11 temperate tree species assessed from forest inventory data. Ann. For. Sci. **69**(2): 195–205. doi:10.1007/s13595-011-0149-0.

Chevan, A., and Sutherland, M. 1991. Hierarchical partitioning. Am. Stat. **45**: 90–96. doi:10.1080/00031305.1991.10475776.

Chu, C.J., Weiner, J., Maestre, F.T., Wang, Y.S., Morris, C., Xiao, S., Yuan, J.L., Du, G.Z., and Wang, G. 2010. Effects of positive interactions, size symmetry of competition and abiotic stress on self-thinning in simulated plant populations. Ann. Bot. **106**(4): 647–652. doi:10.1093/aob/mcq145. PMID:20643802.

Comeau, P.G., White, M., Kerr, G., and Hale, S.E. 2010. Maximum density-size relationships for Sitka spruce and coastal Douglas-fir in Britain and Canada. Forestry, **83**(5): 461–468. doi:10.1093/forestry/cpq028.

Condés, S., Vallet, P., Bielak, K., Bravo-Oviedo, A., Coll, L., Ducey, M.J., Pach, M., Pretzsch, H., Sterba, H., Vayreda, J., and del Río, M. 2017. Climate influences on the maximum size-density relationship in Scots pine (*Pinus sylvestris* L.) and European beech (*Fagus sylvatica* L.) stands. For. Ecol. Manage. **385**: 295–307. doi:10.1016/j.foreco.2016.10.059.

De Martonne, E. 1926. Aréisme et indice artidite. C. R. Acad. Sci., Paris, **182**: 1395–1398.

Deng, J., Wang, G., Morris, E., Wei, X., Li, D., Chen, B., Zhao, C., Liu, J., and Wang, Y. 2006. Plant mass-density relationship along a moisture gradient in north-west China. J. Ecol. **94**(5): 953–958. doi:10.1111/j.1365-2745.2006.01141.x.

Drew, T.J., and Flewelling, J.W. 1979. Stand density management: an alternative approach and its application to Douglas-fir plantations. For. Sci. **25**(3): 518–532.

Gallant, A.R., and Fuller, W.A. 1973. Fitting segmented polynomial regression models whose join points have to be estimated. J. Am. Stat. Assoc. **68**(341): 144–147. doi:10.1080/01621459.1973.10481353.

Harper, J.L. 1977. Population biology of plants. Academic Press, London.

Kweon, D., and Comeau, P.G. 2017. Effects of climate on maximum size-density relationships in Western Canadian trembling aspen stands. For. Ecol. Manage. **406**: 281–289. doi:10.1016/j.foreco.2017.08.014.

Leites, L.P., Robinson, A.P., Rehfeldt, G.E., Marshall, J.D., and Crookston, N.L. 2012. Height-growth response to climatic changes differs among populations of Douglas-fir: a novel analysis of historic data. Ecol. Appl. **22**: 154–165. doi:10.1890/11-0150.1. PMID:22471081.

Lhotka, J.M., and Loewenstein, E.F. 2008. An examination of species-specific growing space utilization. Can. J. For. Res. **38**(3): 470–479. doi:10.1139/X07-147.

Littell, R.C., Milliken, G.A., Stroup, W.W., and Wolfinger, R.D. 1996. SAS system for mixed models. SAS Institute, Inc., Cary, N.C.

Liu, J., Wei, L., Wang, C., Wangl, G., and Wei, X. 2006. Effect of water deficit on self-thinning line in spring wheat (*Triticum aestivum* L.) populations. J. Integr. Plant Biol. **48**(4): 415–419. doi:10.1111/j.1744-7909.2006.00240.x.

Mäkelä, A., and Valentine, H.T. 2006. Crown ratio influences allometric scaling in trees. Ecology, **87**: 2967–2972. doi:10.1890/0012-9658(2006)87[2967:CRIASI]2.0.CO;2. PMID:17249219.

Mäkelä, A., Landsberg, J., Ek, A.R., Burk, T.E., Ter-Mikaelian, M., Ågren, G.I., Oliver, C.D., and Puttonen, P. 2000. Process-based models for forest ecosystem management: current state of the art and challenges for practical implementation. Tree Physiol. **20**(5–6): 289–298. doi:10.1093/treephys/20.5-6.289. PMID:12651445.

Mesfin, D., and Sterba, H. 1996. A yield table model for the growth of *Pinus patula* in Ethiopia. J. Trop. For. Sci. **9**(2): 221–241.

Morris, E.C. 2003. How does fertility of the substrate affect intraspecific competition? Evidence and synthesis from self-thinning. Ecol. Res. **18**(3): 287–305. doi:10.1046/j.1440-1703.2003.00555.x.

Mueller, R.C., Scudder, C.M., Porter, M.E., Talbot Trotter, R., Gehring, C.A., and Whitham, T.G. 2005. Differential tree mortality in response to severe drought: evidence for long-term vegetation shifts. J. Ecol. **93**(6): 1085–1093. doi:10.1111/j.1365-2745.2005.01042.x.

Nally, R.M., and Walsh, C.J. 2004. Hierarchical partitioning public-domain software. Biodivers. Conserv. **13**(3): 659–660. doi:10.1023/B:BIOC.0000009515.11717.0b.

Neumann, M., Mues, V., Moreno, A., Hasenauer, H., and Seidl, R. 2017. Climate variability drives recent tree mortality in Europe. Global Change Biol. **23**(11): 4788–4797. doi:10.1111/gcb.13724.

Newton, P.F. 2012. A decision-support system for forest density management within upland black spruce stand-types. Environ. Modell. Softw. **35**: 171–187. doi:10.1016/j.envsoft.2012.02.019.

Pendry, C.A., and Proctor, J. 1997. Altitudinal zonation of rain forest on Bukit Belalong, Brunei: soils, forest structure and floristics. J. Trop. Ecol. **13**(2): 221–241. doi:10.1017/S0266467400010427.

Peng, C., Ma, Z., Lei, X., Zhu, Q., Chen, H., Wang, W., Liu, S., Li, W., Fang, X., and Zhou, X. 2011. A drought-induced pervasive increase in tree mortality across Canada's boreal forests. Nat. Clim. Change, **1**(9): 467–471. doi:10.1038/nclimate1293.

Pittman, S.D., and Turnblom, E.C. 2003. A study of self-thinning using coupled allometric equations: implications for coastal Douglas-fir stand dynamics. Can. J. For. Res. **33**(9): 1661–1669. doi:10.1139/x03-086.

Poage, N.J., Marshall, D.D., and Mcclellan, M.H. 2007. Maximum stand-density index of 40 western Hemlock-Sitka spruce stands in southeast Alaska. West. J. Appl. For. **22**(2): 99–104.

Pretzsch, H. 2002. A unified law of spatial allometry for woody and herbaceous plants. Plant Biol. **4**(2): 159–166. doi:10.1055/s-2002-25732.

Pretzsch, H. 2006. Species-specific allometric scaling under self-thinning: evidence from long-term plots in forest stands. Oecologia, **146**(4): 572–583. doi:10.1007/s00442-005-0126-0. PMID:16247620.

Pretzsch, H., and Biber, P. 2005. A re-evaluation of Reineke's rule and stand density index. For. Sci. **51**(4): 304–320.

R Development Core Team. 2015. R: a language and environment for statistical computing. R Foundation for Statistical Computing, Vienna, Austria.

Rehfeldt, G.E., Ying, C.C., Spittlehouse, D.L., and Hamilton, D.A. 1999. Genetic responses to climate in *Pinus contorta*: niche breadth, climate change, and reforestation. Ecol. Monogr. **69**(3): 375–407. doi:10.1890/0012-9615(1999)069[0375:GRTCIP]2.0.CO;2.

Reineke, L.H. 1933. Perfecting a stand-density index for even-age forests. J. Agric. Res. **46**(1): 627–638.

Reyes-Hernandez, V., Comeau, P.G., and Bokalo, M. 2013. Static and dynamic maximum size-density relationships for mixed trembling aspen and white spruce stands in western Canada. For. Ecol. Manage. **289**: 300–311. doi:10.1016/j.foreco.2012.09.042.

Rivoire, M., and Le Moguedec, G. 2012. A generalized self-thinning relationship for multi-species and mixed-size forests. Ann. For. Sci. **69**(2): 207–219. doi:10.1007/s13595-011-0158-z.

SAS Institute, Inc. 2011. SAS/STAT 9.3 user's guide. SAS Institute, Inc., Cary, N.C. 3316p.

Schmidt-Vogt, H. 1989. Die Fichte. Bd.II/3: Waldbau, Ökosysteme, Urwald, Wirtschaftswald, Ernährung, Düngung, Ausblick. Verlag Paul Parey, Hamburg. 781 pp.

Segura, G., Balvanera, P., Durán, E., and Pérez, A. 2003. Tree community structure and stem mortality along a water availability gradient in a Mexican tropical dry forest. Plant Ecol. **169**(2): 259–271. doi:10.1023/A:1026029122077.

Shinozaki, K., Yoda, K., Hozumi, K., and Kira, T. 1964. A quantitative analysis of plant form-the pipe model theory: I. Basic analyses. Jpn. J. Ecol. **14**(3): 97–105. doi:10.18960/seitai.14.3_97.

Smith, N.J., and Hann, D.W. 1986. A growth model based on the self-thinning rule. Can. J. For. Res. **16**(2): 330–334. doi:10.1139/x86-056.

Tang, S., Meng, F.R., and Chao, H.M. 1995. The impact of initial stand density and site index on maximum stand density index and self-thinning index in a stand self-thinning model. For. Ecol. Manage. **75**(1–3): 61–68. doi:10.1016/0378-1127(95)03538-L.

Toïgo, M., Vallet, P., Perot, T., Bontemps, J.D., Piedallu, C., and Courbaud, B. 2015. Overyielding in mixed forests decreases with site productivity. J. Ecol. **103**(2): 502–512. doi:10.1111/1365-2745.12353.

Turnblom, E.C., and Burk, T.E. 2000. Modeling self-thinning of unthinned Lake States red pine stands using nonlinear simultaneous differential equations. Can. J. For. Res. **30**(9): 1410–1418. doi:10.1139/x00-072.

VanderSchaaf, C.L., and Burkhart, H.E. 2007. Comparison of methods to estimate Reineke's maximum size-density relationship species boundary line slope. For. Sci. **53**(3): 435–442.

VanderSchaaf, C.L., and Burkhart, H.E. 2008. Using segmented regression to estimate stages and phases of stand development. For. Sci. **54**(2): 167–175.

Vizcaíno-Palomar, N., Ibáñez, I., González-Martínez, S.C., Zavala, M.A., and Alía, R. 2016. Adaptation and plasticity in aboveground allometry variation of four pine species along environmental gradients. Ecol. Evol. **6**(21): 7561–7573. doi:10.1002/ece3.2153.

Vygodskaya, N.N., Schulze, E.D., Tchebakova, N.M., Karpachevskii, L.O., Kozlov, D., Sidorov, K.N., Panfyorov, M.I., Abrazko, M.A., Shaposhnikov, E.S., and Solnzeva, O.N. 2002. Climatic control of stand thinning in unmanaged spruce forests of the southern taiga in European Russia. Tellus B, **54**(5): 443–461. doi:10.3402/tellusb.v54i5.16680.

Wang, T., Hamann, A., Spittlehouse, D.L., and Murdock, T.Q. 2012. ClimateWNA—high-resolution spatial climate data for western North America. J. Appl. Meteorol. Climatol. **51**: 16–29. doi:10.1175/JAMC-D-11-043.1.

Weaver, P.L., and Murphy, P.G. 1990. Forest structure and productivity in Puerto Rico's Luquillo Mountains. Biotropica, **22**(1): 69–82. doi:10.2307/2388721.

Weiskittel, A., Gould, P., and Temesgen, H. 2009. Sources of variation in the self-thinning boundary line for three species with varying levels of shade tolerance. For. Sci. **55**(1): 84–93.

White, J., and Solbrig, O.T. 1980. Demographic factors in populations of plants. *In* Demography and evolution in plant populations. *Edited by* O.T. Solbrig. Blackwell Scientific Publications, Oxford, UK. pp. 21–48.

Woodall, C.W., Miles, P.D., and Vissage, J.S. 2005. Determining maximum stand density index in mixed species stands for strategic-scale stocking assessments. For. Ecol. Manage. **216**(1–3): 367–377. doi:10.1016/j.foreco.2005.05.050.

Worrall, J.J., Rehfeldt, G.E., Hamann, A., Hogg, E.H., Marchetti, S.B., Michaelian, M., and Gray, L.K. 2013. Recent declines of *Populus tremuloides* in North America linked to climate. For. Ecol. Manage. **299**: 35–51. doi:10.1016/j.foreco.2012.12.033.

Wu, Z. 1984. Chinese fir. China Forestry Publishing House, Beijing, China.

Yoda, K. 1963. Self-thinning in overcrowded pure stands under cultivated and natural conditions (intraspecific competition among higher plants XI). J. Biol., Osaka City Univ. **14**: 107–129.

Zeide, B. 1987. Analysis of the 3/2 power law of self-thinning. For. Sci. **33**(2): 517–537.

Zhang, Q., Zhang, L., Weiner, J., Tang, J., and Chen, X. 2011. Arbuscular mycorrhizal fungi alter plant allometry and biomass-density relationships. Ann. Bot. **107**(3): 407–413. doi:10.1093/aob/mcq249. PMID:21169608.

Zhang, X., Duan, A., and Zhang, J. 2013. Tree biomass estimation of Chinese fir (*Cunninghamia lanceolata*) based on Bayesian method. PLoS One, **8**(11): e79868. doi:10.1371/journal.pone.0079868. PMID:24278198.

Zhang, X., Lei, Y., Pang, Y., Liu, X., and Wang, J. 2014. Tree mortality in response to climate change induced drought across Beijing, China. Clim. Change, **124**(1–2): 179–190. doi:10.1007/s10584-014-1089-0.

Zhang, X., Cao, Q.V., Duan, A., and Zhang, J. 2016. Self-thinning trajectories of Chinese fir plantations in southern China. For. Sci. **62**(6): 594–599. doi:10.5849/forsci.16-004.

Zhang, X., Cao, Q.V., Duan, A., and Zhang, J. 2017. Modeling tree mortality in relation to climate, initial planting density, and competition in Chinese fir plantations using a Bayesian logistic multilevel method. Can. J. For. Res. **47**(9): 1278–1285. doi:10.1139/cjfr-2017-0215.

Żywiec, M., Muter, E., Zielonka, T., Delibes, M., Calvo, G., and Fedriani, J.M. 2017. Long-term effect of temperature and precipitation on radial growth in a threatened thermo-Mediterranean tree population. Trees, **31**(2): 491–501. doi:10.1007/s00468-016-1472-8.